Genetic and Physical Mapping of the Mouse *Ulnaless* Locus

Catherine L. Peichel,* Catherine M. Abbott[†,1] and Thomas F. Vogt*

**Department of Molecular Biology, Princeton University, Princeton, New Jersey 08544 and [†]MRC Human Genetics Unit, Western General Hospital, Edinburgh EH4 2XU, Scotland*

Manuscript received June 21, 1996
Accepted for publication September 9, 1996

ABSTRACT

The mouse *Ulnaless* locus is a semidominant mutation which displays defects in patterning along the proximal-distal and anterior-posterior axes of all four limbs. The first *Ulnaless* homozygotes have been generated, and they display a similar, though slightly more severe, limb phenotype than the heterozygotes. To create a refined genetic map of the *Ulnaless* region using molecular markers, four backcrosses segregating *Ulnaless* were established. A 0.4-cM interval containing the *Ulnaless* locus has been defined on mouse chromosome 2, which has identified *Ulnaless* as a possible allele of a *Hoxd* cluster gene(s). With this genetic map as a framework, a physical map of the *Ulnaless* region has been completed. Yeast artificial chromosomes covering this region have been isolated and ordered into a 2 Mb contig. Therefore, the region that must contain the *Ulnaless* locus has been defined and cloned, which will be invaluable for the identification of the molecular nature of the *Ulnaless* mutation.

THE vertebrate limb serves as an experimental paradigm to investigate the translation of gene action into pattern. Classical embryological studies have led to the identification of regions of morphogenetic activity important for the patterning of the limb. Recent molecular and genetic studies of limb mutants have identified molecules associated with these activities (JOHNSON *et al.* 1994; TICKLE 1995; LYON *et al.* 1996).

The mouse *Ulnaless* mutation was identified at Harwell, UK, as a dominant, radiation-induced mutation, with no observed cytogenetic alterations (MORRIS 1967; DAVISSON and CATTANACH 1990). *Ulnaless* heterozygotes are characterized by reductions of the ulna and radius of the forelimb, and malformations of the fibula and tibia of the hindlimb. These mice survive to adulthood, with no other reported malformations. In prior studies, *Ul*/+ males failed to breed; therefore, the homozygous phenotype had not been described (DAVISSON and CATTANACH 1990).

The loss of intermediate limb structures in *Ulnaless* mutants suggests that the locus is important for establishing positional identity along the proximal-distal axis. Information for patterning along this axis appears to reside in the highly proliferative, undifferentiated mesoderm underlying the apical ectodermal ridge, termed the progress zone. The progress zone model proposed by SUMMERBELL *et al.* (1973) posits that positional value along the proximal-distal axis is controlled by the number of cell divisions a cell undergoes in the progress zone, and that these positional values are fixed once the cells leave the progress zone. There is also a more severe reduction of posterior limb structures (ulna and fibula) than anterior structures (radius and tibia) in *Ulnaless* limbs. The anterior-posterior aspect of the *Ulnaless* phenotype is reminiscent of a targeted mutation in the *Wnt7a* gene, which causes a loss of posterior limb structures, such as the ulna and posterior digits, in addition to a loss of dorsal identity (PARR and MCMAHON 1995). Proliferation and patterning of the dorsal-ventral and anterior-posterior axes appears to be coordinated through *sonic hedgehog* (*Shh*) (PARR and MCMAHON 1995; YANG and NISWANDER 1995). Anterior-posterior and proximal-distal patterning may also be linked through *Shh*, which is involved in a positive feedback loop with *Fgf-4* and *Fgf-8* in the apical ectodermal ridge (LAUFER *et al.* 1994; CROSSLEY *et al.* 1996). Identification of the molecular nature of the *Ulnaless* mutation may lead to further insight into the coordination of cell proliferation and patterning along these two axes of the developing limb.

MATERIALS AND METHODS

Mice: *Ulnaless* first arose in the offspring of an irradiated (C3H/HeH × 101/H) male (DAVISSON and CATTANACH 1990). It is now maintained at The Jackson Laboratory on the B6C3HF$_1$ background. Three backcrosses were generated at Princeton and one in Edinburgh. For the intraspecific backcross, *Ul*/+ (B6C3H) females (The Jackson Laboratory, Bar Harbor, ME) were mated to FVB/N males (Taconic, Germantown, NY), and resulting *Ul*/+ F$_1$ females were backcrossed to FVB/N males. The first Princeton intersubspecific backcross was established by mating *Ul*/+ (B6C3H) females to CAST/Ei males, and resulting *Ul*/+ F$_1$ females were backcrossed to C57BL/6J males. The second Princeton intersubspecific backcross was established by mating *Ul*/+ (B6C3H)

Corresponding author: Thomas F. Vogt, 147 Lewis Thomas Lab, Department of Molecular Biology, Princeton University, Princeton, NJ 08544. E-mail: tvogt@watson.princeton.edu

[1]*Present address:* Human Genetics Unit, Department of Medicine, University of Edinburgh, Molecular Medicine Centre, Western General Hospital, Edinburgh EH4 2XU, Scotland.

females to MOLF/Ei males, and resulting *Ul*/+ F_1 males and one resulting F_1 female were backcrossed to C57BL/6J females and males. The Edinburgh intersubspecific backcross was established by mating *Ul*/+ (CBA) females (MRC Radiobiology Unit, Harwell, UK) to CAST/Ei males, and seven resulting F_1 females were backcrossed to CBA males. N_2 offspring were killed at 6 wk of age and scored for the *Ulnaless* limb phenotype, coat color, and sex. Liver and spleen from each mouse was frozen, and DNA was prepared from a piece of the tail.

Skeletal analysis: Newborn mice were stained using alizarin red S and alcian blue 8GX to visualize bone and cartilage, exactly as described by O'BRIEN *et al.* (1996). There were 27 +/+, 45 *Ul*/+, and 22 *Ul*/*Ul* skeletons analyzed from the (*Ul*/+ × FVB/N) F_1 intercross, and five +/+, 9 *Ul*/+, and six *Ul*/*Ul* skeletons analyzed from the (*Ul*/+ × MOLF/Ei) F_1 intercross.

Simple sequence length polymorphisms: All primers for the MIT SSLP markers were purchased from Research Genetics, Huntsville, Alabama (DIETRICH *et al.* 1996). Oligonucleotides *D2Tfv9F* (5′ CTGTGATCCAGCAGTGCTGG 3′) and *D2Tfv9R* (5′ TGCTCTTAGACTCCTACTGC 3′) were designed to flank a trinucleotide repeat 3′ of the *Hoxd-11* gene (GERARD *et al.* 1993), which is the same locus defined by *D2Mit271*. Oligonucleotides *D2Tfv4F* (5′ TGTCTGCCTGCCTGTATCG 3′) and *D2Tfv4R* (5′ CCAGGGGTGcTTGGGAATC 3′) amplify a 160 bp fragment of the *D2Hun5* locus, an interspersed repeat PCR product obtained from Kent Hunter (MCCARTHY *et al.* 1995). Primers Evx2F (5′ CTGCACCGCTCAAGGAAAAC 3′) and Evx2R (5′ GGAGCCGCTCTCCGTGTA 3′) amplify a 700-bp product across the first intron of *Evx-2* (DUSH and MARTIN 1992). Digestion of the PCR product with *Hin*fI yields polymorphic products.

Single-strand conformation polymorphisms (SSCP): Oligonucleotides *D2Tfv3F* (5′ GGACAGCGTCTGAGACTTGA 3′) and *D2Tfv3R* (5′ TCAGGTCGGAATTGAGGC 3′) amplify a 237-bp fragment in the 3′ untranslated region of the *Dlx-2* gene (ROBINSON *et al.* 1991). The previously published *D2Tfv15F* (TV110) and *D2Tfv15R* (TV111) primers are in the third intron of the *Mdk* gene (PEICHEL *et al.* 1993). Oligonucleotides *D2Tfv13F* (5′ CTGAGGCCCACTCTTAAGGC 3′) and *D2Tfv13R* (5′ ACCTTTCCTCCCCATGAGG 3′) amplify a 242-bp product and oligonucleotides *D2Tfv14F* (5′ ATTCTCGGGTGCAGAGTGG 3′) and *D2Tfv14R* (5′ CACACGAAGAGGTAGGAGCG 3′) amplify a 226-bp product in the 3′ untranslated region of the *Hoxd-1* gene (FROHMAN and MARTIN 1992). SSCP was carried out as previously described (PEICHEL *et al.* 1993).

***Y* chromosome genotyping:** Primers to the mouse *Y* chromosome specific *Zfy* gene were as published (NAGAMINE *et al.* 1989).

Statistical analysis: Recombination frequencies and 95% confidence intervals were determined with a confidence interval calculation program developed by Lee Silver (SILVER 1995). The *P* values were calculated using the CHIDIST function of Microsoft Excel 5.0.

Genomic PFGE mapping: Large molecular weight genomic DNA was prepared from the spleens of 2-mon-old +/+, *Ul*/+ and *Ul*/*Ul* mice and digested with *Sfi*I. PFGE was carried out on a Bio-Rad CHEF mapper, to separate between 200 and 1000 kb. The same blot was repetitively probed with the *Hoxd-1, Hoxd-9, Hoxd-11, Hoxd-12,* and *Hoxd-13* genes. The *Hoxd-1* probe is an 831-bp PCR fragment containing the homeodomain and 3′ untranslated region, and it was generated using oligonucleotides *D2Tfv14′F* (5′ GAATATGGAGCCACAAGCCC 3′) and *D2Tfv14R* (FROHMAN and MARTIN 1992). The *Hoxd-9, Hoxd-11, Hoxd-12,* and *Hoxd-13* probes were obtained from P. CHAMBON (DUBOULE and DOLLE 1989; DOLLE *et al.* 1991; IZPISUA-BELMONTE *et al.* 1991).

Yeast artificial chromosome (YAC) library screening: Both the Princeton and MIT YAC libraries (ROSSI *et al.* 1992; KUSUMI *et al.* 1993) were screened by PCR for the *Hoxd-1, Hoxd-9,* and *Evx-2* genes as well as for microsatellite markers *D2Mit10* and *D2Mit247*. Oligonucleotides *D2Tfv13F* and *D2Tfv13R* were used to screen both libraries for the *Hoxd-1* gene. Oligonucleotides *D2Tfv11F* (5′ GTCTTGTCCTGTCCCACTCC 3′) and *D2Tfv11R* (5′ CTCGGAATTAGATCGTTGGC 3′) amplify a 186-bp fragment in the 3′ untranslated region of the *Hoxd-9* gene (RENUCCI *et al.* 1992) and were used to screen the Princeton library. Oligonucleotides *D2Tfv10F* (5′ TGTCGAGGGTTTACATGTGG 3′) and *D2Tfv10R* (5′ CCTCGCCTCTTTTCTTACCT 3′) amplify a 276-bp fragment 5′ of the *Hoxd-9* gene (RENUCCI *et al.* 1992) and were used to screen the MIT library. Oligonucleotides *D2Tfv7F* (5′ CAAGGTATCGATTCCAGCGC 3′) and *D2Tfv7R* (5′ AAGCACCGACCTTGGGATTC 3′) amplify a 232-bp product in the second intron of the *Evx-2* gene (P. GRUSS, unpublished sequence).

YAC sizing: To prepare large molecular weight yeast DNA for pulsed field gel electrophoresis (PFGE), the protocol of CARLE and OLSON (1985) was used. PFGE was carried out on a Bio-Rad CHEF mapper, separating between 200 and 2000 kb. To determine YAC size and to see if they contained both arms, duplicate filters were probed with the 2672-bp *Bam*HI-*Pvu*II and the 1689-bp *Bam*HI-*Pvu*II fragments of pBR322, which recognize the left and right arms of pYAC4, respectively.

YAC end isolation: To obtain YAC DNA for end rescue, Southern blot analysis, and PCR, the protocol of HOFFMAN and WINSTON (1987) was used. Ends of YACs were isolated according to a protocol modified from OCHMAN *et al.* (1988). For the left arm, *Taq*I, *Sau*3A, and *Hae*III were used, and for the right arm, *Hha*I, and *Hae*III were used. For the left end rescue, primers 5L (5′ GTTTAAGGCGCAAGACTT 3′) and 5R′ (5′ TCCTTCCAAGATGGTTCAGAGT 3′) were used. For right end rescue primers R7 (5′ TTCAAGAATTGATCCTCTACGC 3′) and 3R (5′ TCTCAAGATTACGGAAT 3′) were used. YACs FF1.F4, FFC.C8, and FDZ.A3 yielded positive left ends of 560, 990, and 640 bp with *Taq*I, while AAR.F5 yielded a positive left end of 870 bp with *Sau*3A.

YAC mapping: Positive ends were subcloned into the TA cloning vector pCRII (Invitrogen). Plasmid DNA was prepared using the CTAB protocol (DEL SAL *et al.* 1989). Ends were sequenced using the TAF (5′ GATCCACTAGTAACGGCC 3′) and TAR (5′ GAGCGGCCGCCAGTGTGA 3′) oligonucleotides complementary to the TA vector sequence surrounding the cloning site. Oligonucleotides *D2Tfv6F* (5′ ATTCACACAGGTGCACATGC 3′) and *D2Tfv6R* (GTAGGCACAACCCAGGTAGG 3′) amplify a 104-bp fragment flanking a $(CA)_n$ repeat in the left end of YAC FF1.F4. Oligonucleotides *D2Tfv5F* (5′ TGCTGACTACATCCTTAAGTGC 3′) and *D2Tfv5R* (5′ GTCCTCAACTACCAAGCTGC 3′) amplify a 131-bp fragment in the left end of YAC FFC.C8. For PCR content mapping, all of the YACs were screened for the presence of *D2Mit10, D2Mit158, D2Mit219, D2Mit247, D2Mit299, D2Mit418,* and *D2Mit435, D2Hun5* (*D2Tfv4*), *Hoxd-1* (*D2Tfv13*; *D2Tfv14*), *Hoxd-4* (*D2Tfv12*), *Hoxd-9* (*D2Tfv10*; *D2Tfv11*), *Hoxd-10* (*D2Mit37*), *Hoxd-11* (*D2Tfv9*), *Hoxd-12* (*D2Tfv8*), and *Evx-2* (*D2Tfv7*). Oligonucleotides *D2Tfv12F* (5′ TCTAGGTTGAGCGAAGCTGC 3′) and *D2Tfv12R* (5′ TTCCCCACTTTAGGGAGGG 3′) amplify a 151-bp fragment in the 3′ UTR of *Hoxd-4* (FEATHERSTONE *et al.* 1988), *D2Mit37* amplifies a 140-bp fragment in the intron of *Hoxd-10* (RENUCCI *et al.* 1992), and oligonucleotides *D2Tfv8F* (5′ AGTTGGACAGGGAGGAGACC 3′) and *D2Tfv8R* (5′ GAGGTG-

GGAGCGAAATCT 3′) amplify a 442-bp fragment, including the homeodomain, of the *Hoxd-12* gene (IZPISUA-BELMONTE *et al.* 1991).

RESULTS

Generation of homozygotes: Although *Ul*/+ females are fertile, previous studies had noted that *Ul*/+ males failed to breed; therefore, homozygotes had not been described (DAVISSON and CATTANACH 1990). Although +/+ (B6C3H) females and *Ul*/+ (B6C3H) males were caged together for a 6-mon period, no pups were ever born. Daily examination over a month showed no vaginal plugs; however, sperm from *Ul*/+ males was found to be normal in number and motility, suggesting either a behavioral or a physical impediment to mating (C. L. PEICHEL and T. F. VOGT, unpublished observations). Following *in vitro* fertilization with sperm from *Ul*/+ males and eggs from +/+ females, *Ulnaless* offspring were obtained. We sought to increase breeding vigor by placing *Ul*/+ males on a different genetic background. *Ul*/+ (B6C3H) females were mated to FVB/N and MOLF/Ei males. The resulting (*Ul*/+ × FVB/N) F_1 and (*Ul*/+ × MOLF/Ei) F_1 males bred, albeit with reduced fecundity.

Limb phenotype: (*Ul*/+ × FVB/N) F_1 and (*Ul*/+ × MOLF/Ei) F_1 mice were reciprocally intercrossed to determine the homozygous phenotype. A trinucleotide repeat in the closely linked *Hoxd-11* gene was used to genotype all offspring in the (*Ul*/+ × FVB/N) *Ul*/+ and (*Ul*/+ × MOLF/Ei) *Ul*/+ intercrosses. Both heterozygotes and homozygotes were present at birth.

To investigate the skeletal phenotype of *Ulnaless* neonates, we performed alcian blue/alizarin red staining. No abnormalities of the axial or cranial skeleton were detected in *Ul*/+ or *Ul*/*Ul* mice on the FVB/N or MOLF/Ei backgrounds. However, the intermediate elements of all four limbs of these animals were uniformly affected (Figure 1). The most striking defect is the severe reduction of the ulna and radius in the forelimbs. *Ul*/*Ul* animals have slightly more severe defects than *Ul*/+ animals (Figure 1). The radius of *Ul*/*Ul* forelimbs appears to be reduced relative to the *Ul*/+ forelimbs, leading to the loss of the space that is normally present between the ulna and radius of *Ul*/+ animals. In addition, the ossification center of the ulna is not present in neonatal *Ul*/*Ul* forelimbs. In the hindlimbs, there is a severe loss of the fibula and a less severe reduction and bowing of the tibia. The hindlimbs of *Ul*/+ and *Ul*/*Ul* mice are similar except that the ossification center in the fibula is not seen at this stage in the *Ul*/*Ul* hindlimbs. The lack of such a center at this stage seems to be due to a delay in ossification.

Perinatal lethality: At birth, the expected 1:2:1 ratio of +/+:*Ul*/+:*Ul*/*Ul* genotypes was obtained in both the FVB/N and MOLF/Ei intercrosses (Table 1). However, in the FVB/N intercross, very few *Ul*/*Ul* animals were found at weaning (Table 1). Interestingly, the 14 surviving homozygotes were all males as determined phenotypically and as genotyped by PCR for *Zfy*, a *Y* chromosome specific marker (NAGAMINE *et al.* 1989). Therefore, in the FVB/N backcross, both *Ul*/*Ul* males and females are born, but females do not survive and males rarely survive to weaning. In contrast, both *Ul*/*Ul* males and females survive to weaning in the MOLF/Ei intercross (Table 1).

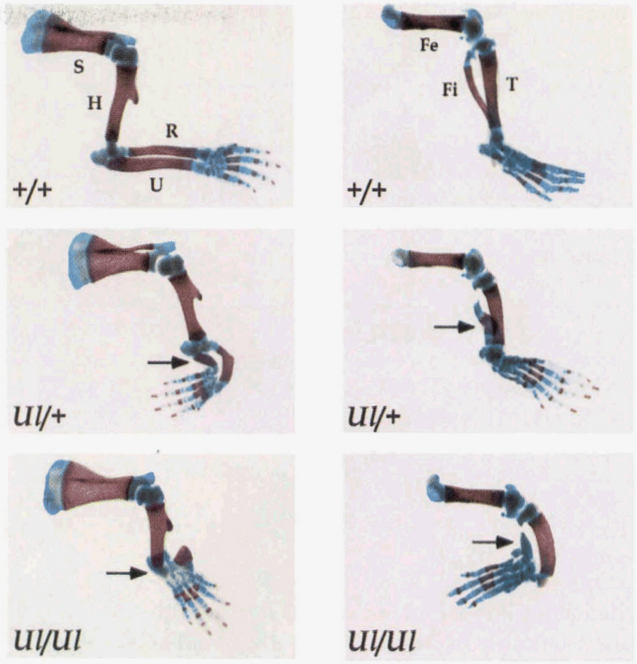

FIGURE 1.—The *Ulnaless* limb phenotype. Alizarin red/alcian blue skeletal staining of neonatal +/+, *Ul*/+ and *Ul*/*Ul* forelimbs (left) and hindlimbs (right) are shown. The scapula (S), humerus (H), radius (R), and ulna (U) are indicated on the wild-type forelimb and the femur (Fe), tibia (T) and fibula (F) are indicated on the wild-type hindlimb. Arrows point to the ossification center present in the *Ul*/+ ulna, but not in the *Ul*/*Ul* ulna, and the ossification center present in the *Ul*/+ fibula, but not in the *Ul*/*Ul* fibula.

There was also evidence for perinatal lethality in the backcrosses. In the FVB/N backcross, there is a significant deviation at weaning from the expected 1:1 ratio of +/+:*Ul*/+ animals. Both male and female *Ulnaless* heterozygotes are reduced relative to wild type (Table 2). In both the Princeton and Edinburgh CAST/Ei backcrosses, there is a significant decrease in *Ul*/+ females from the expected 1:1 ratio of +/+:*Ul*/+ females (Table 2). There were no deviations from the expected 1:1 ratio of +/+:*Ul*/+ animals for either males or females in the MOLF/Ei backcross (Table 2). A deficiency of *Ulnaless* heterozygote females has previously been observed in maintenance crosses on the B6C3H background at The Jackson Laboratory, and a deficiency of *Ul*/+ males and females was observed in maintenance crosses at Harwell (DAVISSON and CATTANACH 1990). Taken together with the lethality of *Ul*/*Ul* animals observed in the intercrosses, these data suggest

TABLE 1

Homozygote lethality

Intercross	Age	+/+			*Ul*/+			*Ul*/*Ul*		
		M	F	Total	M	F	Total	M	F	Total
FVB/N	Birth[a]	7	20	27	16	29	45	8	14	22
	Weaning[b]	34	39	73	72	59	131	14	0	14
MOLF/Ei	Birth[c]	1	4	5	6	3	9	2	2	4
	Weaning[d]	8	8	16	17	15	32	12	5	17

All progeny generated in the (*Ul*/+ × FVB/N) *Ul*/+ and (*Ul*/+ × MOLF/Ei) *Ul*/+ intercrosses were genotyped for the *Ulnaless* locus by the *Hoxd-11* trinucleotide repeat marker (GERARD *et al.* 1993). For progeny killed at birth, the number of males (M) and females (F) was determined by PCR with the *Zfy* marker (NAGAMINE *et al.* 1989). For progeny analyzed at weaning, sex was determined by external morphological observation. Based on the null hypothesis of a 1:2:1 ratio of +/+: *Ul*/+: *Ul*/*Ul* progeny, we calculated the following:

[a] $\chi^2 = 2.4$, 2 d.f., $P = 0.30$.
[b] $\chi^2 = 49.2$, 2 d.f., $P = 2.0 \times 10^{-7}$.
[c] $\chi^2 = 0.3$, 2 d.f., $P = 0.86$.
[d] $\chi^2 = 0.06$, 2 d.f., $P = 0.97$.

that there is sex and strain specific, semidominant perinatal lethality associated with the *Ulnaless* mutation.

Genetic mapping: *Ulnaless* had been mapped in a large genetic interval, 18 cM proximal to *pallid* and 32 cM proximal to *agouti* on mouse chromosome *2* (DAVISSON and CATTANACH 1990; SIRACUSA *et al.* 1995). To map *Ulnaless* in relation to molecular markers, we established an intraspecific backcross with FVB/N, two intersubspecific backcrosses with CAST/Ei, and one intersubspecific backcross with MOLF/Ei, generating 513, 344, 549 and 158 N_2 progeny, respectively. By testing all of the 21 MIT SSLPs (DIETRICH *et al.* 1996) in a 4.5 cM interval flanking *Ulnaless,* we found that there was a 38% polymorphism rate between the *Ul*/+ (B6C3H) and FVB/N strains, and a 76% polymorphism rate between the *Ul*/+ (B6C3H) and CAST/Ei or MOLF/Ei strains.

TABLE 2

Segregation of N_2 mice by phenotype and sex

Backcross	Females		Males	
	+/+	*Ul*/+	+/+	*Ul*/+
FVB/N[a]	145	88	163	117
CAST/Ei[b]	85	57	95	107
CAST/Ei[c]	143	111	153	142
MOLF/Ei[d]	35	41	41	41

N_2 animals were scored for sex and phenotype by external morphological observation at 6 wk of age.

[a] (*Ul*/+ × FVB/N) × FVB/N, based on the null hypothesis of 1:1 +/+: *Ul*/+ animals, $\chi^2 = 34.4$, 1 d.f., $P = 4.5 \times 10^{-9}$.
[b] (*Ul*/+ × CAST/Ei) × C57BL/6J, based on the null hypothesis of 1:1 +/+: *Ul*/+ females, $\chi^2 = 9.2$, 1 d.f., $P = 2.4 \times 10^{-3}$.
[c] (*Ul*/+ × CAST/Ei) × CBA, based on the null hypothesis of 1:1 +/+: *Ul*/+ females, $\chi^2 = 7.2$, 1 d.f., $P = 7.5 \times 10^{-3}$.
[d] (*Ul*/+ × MOLF/Ei) × C57BL/6J, based on the null hypothesis of 1:1 +/+: *Ul*/+ animals, $\chi^2 = 0.44$, 1 d.f., $P = 0.51$.

In testing markers on chromosome *2* for polymorphisms, we found that the markers *D2Mit92, D2Mit328, D2Mit247,* and *D2Mit418* were polymorphic between *Ul*/+ (B6C3H) and +/+ (B6C3H) animals. As the *Ulnaless* mutation arose in an irradiated (C3H/HeH × 101/H) male (DAVISSON and CATTANACH 1990), we tested to see if the *Ul* allele segregated with C3H/HeH or 101/H. *Ul* segregates with the 101/H allele in all cases.

By scoring the 513 N_2 progeny of the FVB/N backcross for molecular markers on mouse chromosome *2,* we refined the *Ul* region to a 2.0 cM interval between *D2Mit328* and *D2Mit93* (Figure 2A; Table 3A). None of the other MIT markers in this interval were found to be polymorphic in the FVB/N cross. Therefore, all the markers in the interval from *D2Mit11* to *D2Mit159* were scored, where possible, in the 344 N_2 progeny of the Princeton CAST/Ei backcross, the 549 N_2 progeny of the Edinburgh CAST/Ei backcross, and the 158 N_2 progeny of the MOLF/Ei backcross (Figure 2, B–D; Table 3, B–D). We were able to define a 0.4-cM region encompassing the *Ulnaless* locus. *D2Mit10* was scored in the 505 N_2 progeny of the Princeton CAST/Ei and MOLF/Ei backcrosses, and it was found to lie 0.2 cM proximal to *Ul. D2Mit219* was scored in the 1051 N_2 progeny of all three intersubspecific backcrosses, and it was found to be 0.2 cM distal to *Ul.*

We also anchored markers from our crosses in The Jackson Laboratory interspecific backcross panels (ROWE *et al.* 1994; THE JACKSON LABORATORY BACKCROSS DNA PANEL, 1996). *D2Mit247* and *D2Mit418* did not recombine with *Ul* or *Hoxd-11* in our crosses, but in the Jackson BSB cross, we were able to place *D2Mit247* and *D2Mit418* distal to *Hoxd-11,* which was useful for our physical mapping (see below). Additionally, we were able to rule out genes that have been mapped in these panels as candidates for *Ulnaless.* For instance, *Acra* is mapped proximal to *D2Mit10* in the

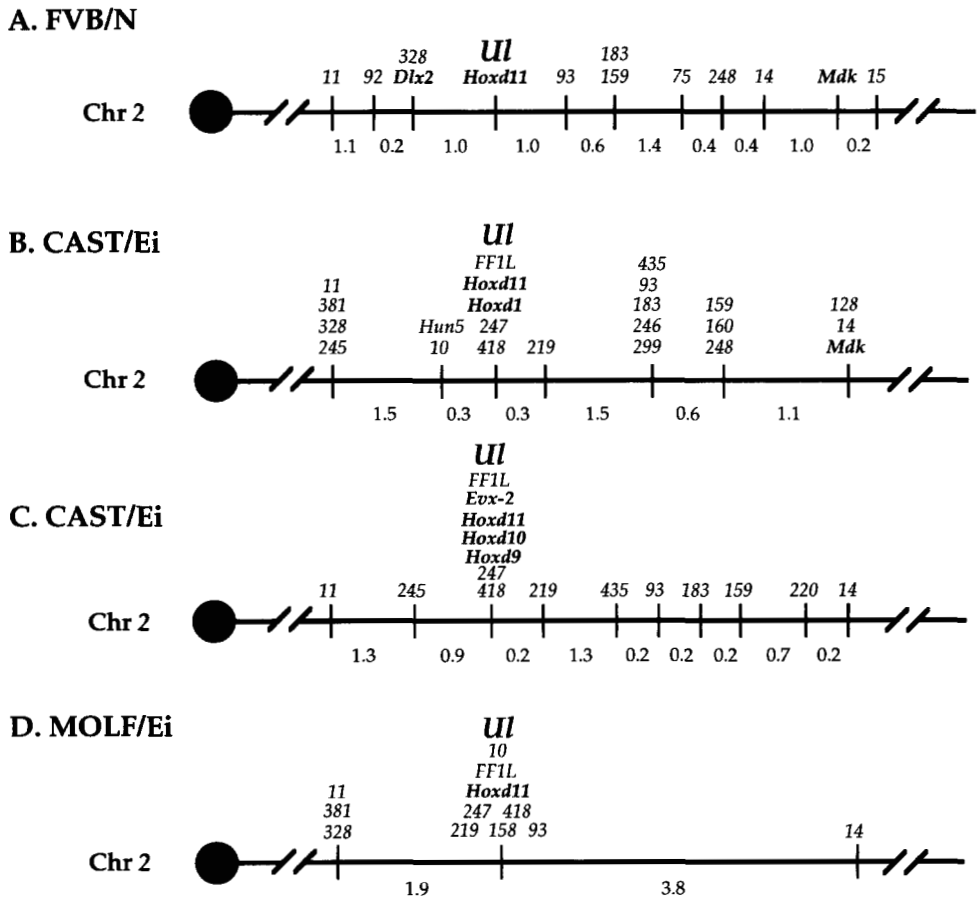

FIGURE 2.—Genetic mapping of the *Ulnaless* locus. The position of loci scored on mouse chromosome *2* in (A) 513 N_2 progeny of the FVB/N backcross, (B) 344 N_2 progeny of the Princeton CAST/Ei backcross, (C) 549 N_2 progeny of the Edinburgh CAST/Ei backcross, and (D) 158 N_2 progeny of the MOLF/Ei backcross. All the numbered loci refer to the MIT SSLP markers. Recombination distances between loci are shown in cM below the schematic chromosome where the ball indicates the centromere.

Jackson BSS cross, and we know that *D2Mit10* defines the proximal boundary of the *Ulnaless* locus. An interspersed repetitive sequence PCR product, *D2Hun5* (MCCARTHY *et al.* 1995) was localized to the *Ulnaless* region in the Jackson BSS cross. An SSLP in *D2Hun5* was used to map it in the Princeton CAST/Ei backcross. This marker, together with *D2Mit10,* defined the proximal boundary of the *Ulnaless* region (Figure 2B, Table 3B).

To compare the distances between loci in multiple crosses, five anchor loci (*D2Mit11, D2Mit328, Hoxd-11, D2Mit93,* and *D2Mit14*) were scored, wherever possible, in our four backcrosses and in The Jackson Laboratory backcrosses (Table 4). The *Ulnaless* and community interspecific backcrosses were generated through the female F_1 except for 111 N_2 progeny in the MOLF/Ei backcross, which were generated through F_1 males. The overall distance between flanking markers *D2Mit11* and *D2Mit14* was very similar in all the crosses, with a range of 4.3–7.4 cM. However, variation in the location of recombination events was observed for both different strains and different sexes. Particularly striking is the difference between the location of recombination events in male and female meiosis in the MOLF/Ei backcross. We observe a distance of 4.3 cM from *D2Mit328* to *Hoxd-11* in the female F_1 and a distance of 0.9 cM in the male F_1 mice. Recombination did not occur between *Hoxd-11* and *D2Mit14* in the female F_1, but it did occur between these same markers in the male F_1 mice, giving a distance of 5.4 cM.

Relative order between markers was conserved in all the crosses we scored. However, comparison of our data to the MIT CAST/Ei intercross (DIETRICH *et al.* 1996) showed two discrepancies. First, *D2Mit10* was previously mapped proximal to *D2Mit11* in the MIT CAST/Ei intercross. We place *D2Mit10* distal to *D2Mit11* in the Princeton CAST/Ei and MOLF/Ei backcrosses, as well as in The Jackson Laboratory backcrosses (Figure 2, B and D). Placement of *D2Mit10* on YACs from the *Ulnaless* region (see below), supports our placement of *D2Mit10* distal to *D2Mit11.* Second, *D2Mit128* was previously mapped proximal to *D2Mit160* and *D2Mit248* in the MIT intercross. We place *D2Mit128* distal to these markers in the Princeton CAST/Ei backcross (Figure 2B).

Candidate gene analysis: A significant advantage of a refined genetic map is its power for assessing candidate genes. Based on their relative map position on mouse chromosome *2,* as well as their expression in the developing limb, we wanted to map *Dlx-1* and *Dlx-2, Mdk,* and the *Hoxd* cluster relative to *Ulnaless* (KADOMATSU *et al.* 1990; DOLLE *et al.* 1992; IZPISUA-BELMONTE and DUBOULE 1992; BULFONE *et al.* 1993, B. PRABHAKARAN, J. L. MORAN, and T. F. VOGT, unpublished observations). *Dlx-1* and *Dlx-2* are within 25 kb of each other; therefore, we initially scored the *Dlx-2* gene relative to *Ul* (SIMEONE *et al.* 1994). We

TABLE 3

Recombination frequencies of *Ulnaless* with flanking markers

Interval	R	*N*	*RF*	95% Conf. limits
A. (*Ul*/+ × FVB/N) × FVB/N				
11-92	1	88	1.1	0.3–6.1
92-(328, Dlx-2)	1	513	0.2	0.1–1.1
(328, Dlx-2)-(Hoxd-11, Ul)	5	513	1.0	0.4–2.3
(Hoxd-11, Ul)-93	5	513	1.0	0.4–2.3
93-(183, 159)	3	513	0.6	0.2–1.7
(183, 159)-75	7	513	1.4	0.7–2.8
75-248	2	513	0.4	0.1–1.4
248-14	2	513	0.4	0.1–1.4
14-Mdk	5	513	1.0	0.4–2.3
Mdk-15	1	513	0.2	0.1–1.1
B. (*Ul*/+ × CAST/Ei) × C57BL/6J				
(11, 381, 328, 245)-(10, Hun5)	5	344	1.5	0.7–3.4
(10, Hun5)-(FF1L, Hoxd-11, d-1, Ul, 247, 418)	1	344	0.3	0.1–1.6
(FF1L, Hoxd-11, d-1, Ul, 247, 418)-219	1	344	0.3	0.1–1.6
219-(435, 93)	5	344	1.5	0.7–3.4
(435, 93)-(183, 246, 299)	0	178	0.0	0.0–2.0
(183, 246, 299)-(159, 160, 248)	1	178	0.6	0.2–3.1
(159, 160, 248)-(128, 14, Mdk)	2	178	1.1	0.4–4.0
C. (*Ul*/+ × CAST/Ei) × CBA				
11-245	7	549	1.3	0.6–2.6
245-(FF1L, Evx-2, Hoxd-11, d-10, d-9, Ul, 247, 418)	5	549	0.9	0.5–2.4
(FF1L, Evx-2, Hoxd-11, d-10, d-9, Ul, 247, 418)-219	1	549	0.2	0.1–1.0
219-435	7	549	1.3	0.6–2.6
435-93	1	549	0.2	0.1–1.0
93-183	1	549	0.2	0.1–1.0
183-159	1	549	0.2	0.1–1.0
159-220	4	549	0.7	0.3–1.9
220-14	1	549	0.2	0.1–1.0
D. (*Ul*/+ × MOLF/Ei) × C57BL/6J and C57BL/6J × (*Ul*/+ × MOLF/Ei)				
(11, 381, 328)-10	3	158	1.9	0.7–5.4
10-(FF1L, Hoxd-11, Ul, 247, 418)	0	158	0.0	0.0–2.3
(FF1L, Hoxd-11, Ul, 247, 418)-(219, 93, 158)	0	158	0.0	0.0–2.3
(219, 93, 158)-14	6	158	3.8	1.8–8.0

Recombination frequencies (*RF*) in centimorgans and 95% confidence limits were calculated from the number of recombinants (R) in a sample size (*N*) using a program developed by Lee Silver (SILVER 1995).

defined SSCPs in the *Dlx-2* and *Mdk* genes, and they were used to score the recombinants in this region (ROBINSON *et al.* 1991; PEICHEL *et al.* 1993). *Dlx-2* was found to be 1.2 cM proximal to the *Ulnaless* locus in the FVB/N backcross (Figure 2A; Table 3A), and *Mdk* was found to be 4.8 cM distal to *Ulnaless* in the FVB/N backcross and 3.5 cM distal to *Ulnaless* in the Princeton CAST/Ei backcross (Figure 2, A and B; Table 3, A and B). Based on recombination, these genes have been ruled out as candidates for *Ulnaless*.

In contrast, a trinucleotide repeat in the *Hoxd-11* gene (GERARD *et al.* 1993) did not recombine with *Ulnaless* in 1564 N_2 animals, demonstrating tight linkage and possible allelism (Table 3, Figure 2). The *Hoxd-11* gene is one of 10 genes in the *Hoxd* cluster, which is in a 100-kb interval (BASTIAN *et al.* 1992). Therefore, we wanted to rule out any of the genes of the *Hoxd* cluster as alleles of *Ulnaless*. We defined a SSCP in the *Hoxd-1* gene to map it relative to *Ul* (FROHMAN and MARTIN 1992). *Hoxd-1* does not recombine with *Ul* in the 344 N_2 animals of the Princeton CAST/Ei cross. In addition, a restriction length variant in the intron of *Evx-2* (DUSH and MARTIN 1992) and SSLPs in *Hoxd-10* and *Hoxd-9* (RENUCCI *et al.* 1992) do not recombine with *Ul* in the 549 N_2 animals of the Edinburgh CAST/Ei cross. Therefore, all 10 genes of the *Hoxd* cluster remain candidates for *Ulnaless*.

Because *Ulnaless* was radiation induced, we looked for alterations of the *Hoxd* locus. Therefore, PFGE was

TABLE 4

Comparison of genetic distances of markers on chromosome *2*

Cross	Interval			
	11-328	*328-Hoxd-11*	*Hoxd-11-93*	*93-14*
FVB/N (female)	1/88 (1.1)	5/513 (1.0)	5/513 (1.0)	14/513 (2.7)
CAST/Ei (female)[a]	0/344 (0.0)	6/344 (1.7)	6/344 (1.7)	3/178 (1.7)
CAST/Ei (female)[b]	ND	12/549 (2.2)[c]	9/549 (1.6)	7/549 (1.3)
MOLF/Ei (female)	0/47 (0.0)	2/47 (4.3)	0/47 (0.0)	0/47 (0.0)
MOLF/Ei (male)	0/111 (0.0)	1/111 (0.9)	0/111 (0.0)	6/111 (5.4)
BSB (female)	1/94 (1.1)	0/94 (0.0)	2/94 (2.1)	ND
BSS (female)	1/94 (1.1)	2/94 (2.1)	1/94 (1.1)	3/94 (3.2)
Total	3/778 (0.4)	28/1752 (1.6)	23/1752 (1.3)	33/1492 (2.2)

A comparison of genetic distances between markers scored in all four *Ulnaless* backcrosses. The genetic distances between these markers in the two Jackson Laboratory interspecific backcrosses (BSB and BSS) are also shown (ROWE *et al.* 1994). Number of recombinants are shown over the number of animals scored. Recombination frequencies (in parentheses) are expressed in centimorgans. *D2Mit328* could not be scored in the Edinburgh CAST/Ei backcross and *D2Mit14* could not be scored in the BSB cross; therefore, these recombination frequencies could not be determined (ND).

[a] (*Ul*/+ × CAST/Ei) × C57BL/6J.

[b] (*Ul*/+ × CAST/Ei) × CBA.

[c] Determined for the interval, *D2Mit11-Hoxd-11.*

carried out on DNA from +/+, *Ul*/+ and *Ul*/*Ul* mice digested with *Mlu*I, *Not*I, *Sma*I, *Sfi*I, and *Xho*I. Using probes for *Hoxd-1, Hoxd-9, Hoxd-11, Hoxd-12,* and *Hoxd-13,* the *Sfi*I digests allowed us to cover the entire *Hoxd* cluster (Figure 3). There were no alterations of the *Hoxd* cluster detected by this analysis. Similarly, genomic Southern analysis using probes for *Hoxd-1, Hoxd-4, Hoxd-8, Hoxd-9, Hoxd-10, Hoxd-11, Hoxd-12, Hoxd-13,* and *Evx-2* did not detect any differences between +/+, *Ul*/+, and *Ul*/*Ul* DNA (C. L. PEICHEL and T. F. VOGT, unpublished observations). Therefore, *Ulnaless* is not due to a large rearrangement of the *Hoxd* cluster.

Physical mapping: In order to clone the physical DNA surrounding the *Ulnaless* locus, we screened the Princeton and MIT YAC libraries (ROSSI *et al.* 1992; KUSUMI *et al.* 1993). We initially screened both libraries with the *Hoxd-9* gene and isolated five YACs (Table 5). C.45.H7, C.91.G12, C.97.E8, and FF1.F4 contained *Hoxd-1, Hoxd-4, Hoxd-9, Hoxd-10, Hoxd-11, Hoxd-12,* and *Evx-2*; however, these YACs did not contain any other markers from the *Ulnaless* genetic interval (Figure 4).

To extend the coverage of the *Ulnaless* region, we next screened both libraries with markers from each end of the *Hoxd* cluster. *Hoxd-1* isolated FDZ.A3 (Table 5), which contained *Hoxd-1, Hoxd-4,* and the 3′ end of *Hoxd-9* but not the 5′ end of *Hoxd-9* (Figure 4). *Evx-2* isolated FFC.C8 (Table 5), which also contains the *Hoxd-12* gene but none of the more 3′ genes of the cluster (Figure 4). Based on the orientation of the human *HOXD* cluster relative to the centromere (ROSSI *et al.* 1994), we assumed that the *Evx-2* YAC extends toward the centromere and *D2Mit10*/*D2Hun5,* and that the *Hoxd-1* YAC extends towards the telomere and *D2Mit247.*

D2Mit10 lies 0.3 cM proximal to the *Ulnaless* locus and was not present on any of the *Hoxd* YACs. We iso-

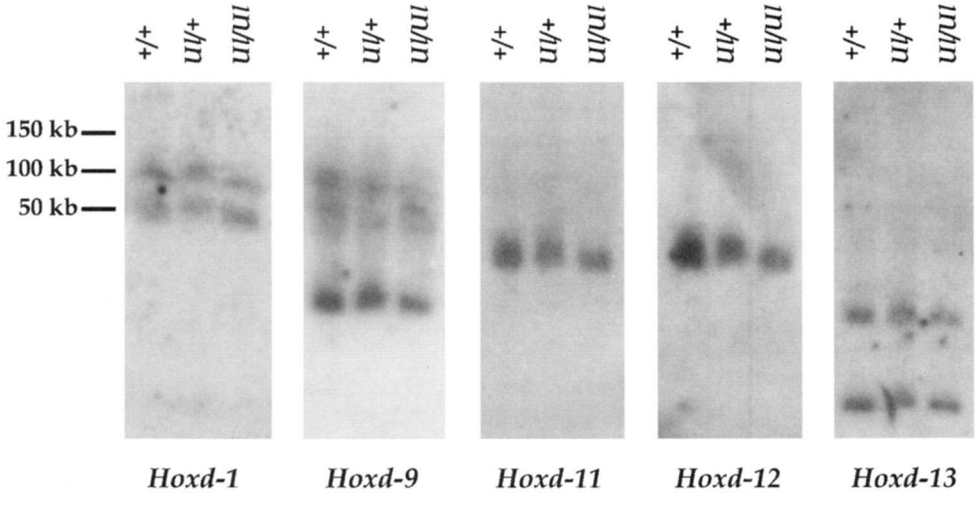

FIGURE 3.—Pulsed-field gel analysis of the *Hoxd* cluster. Large molecular weight DNA from +/+, *Ul*/+ and *Ul*/*Ul* spleens was digested with *Sfi*I and subjected to PFGE. The same blot was repetitively probed with *Hoxd-1, Hoxd-9, Hoxd-11, Hoxd-12,* and *Hoxd-13.* Sizes of the lambda ladder are indicated on the left. The conditions used for this gel did not allow us to accurately size fragments <50 kb.

TABLE 5

YACs spanning the *Ulnaless* locus

YAC	Marker	Library	Size
C.45.H7	*Hoxd-9*	Princeton	245
C.91.G12	*Hoxd-9*	Princeton	290
C.97.E8	*Hoxd-9*	Princeton	220
C.172.A3	*Hoxd-9*	Princeton	245
FF1.F4	*Hoxd-9*	MIT	770
FDZ.A3	*Hoxd-1*	MIT	580
FFC.C8	*Evx-2*	MIT	650
C.91.H10	*D2Mit10*	Princeton	250
D.4.F7	*D2Mit10*	Princeton	290
D.35.G6	*D2Mit10*	Princeton	330
FBU.E9	*D2Mit10*	MIT	700
FCP.F9	*D2Mit10*	MIT	650
FEB.F11	*D2Mit10*	MIT	680
FER.H1	*D2Mit10*	MIT	700
AAR.F5	*D2Mit247*	MIT	500

YACs spanning the *Ulnaless* locus were identified by PCR screening of the Princeton and MIT YAC libraries (Rossi *et al.* 1992; Kusumi *et al.* 1993) with the marker indicated. Sizes in kilobases of the YACs were determined by PFGE analysis.

lated seven new YACs with *D2Mit10* (Table 5), and all contained *D2Hun5*. Because *D2Hun5* does not recombine with *D2Mit10* in the CAST/Ei backcross or the BSS backcross, we cannot order *D2Mit10* and *D2Hun5* relative to each other (Figure 4).

Although *D2Mit247* does not recombine with *Ulnaless* in the CAST/Ei and the MOLF/Ei backcrosses, it is mapped distal to *Hoxd-11* in the BSB backcross. We isolated YAC AAR.F5 with *D2Mit247* (Table 5). This YAC also contained *D2Mit418*, which does not recombine with *D2Mit247* in the CAST/Ei, MOLF/Ei, or The Jackson Laboratory backcrosses. Importantly, it contains *D2Mit219*, which recombines with *Ulnaless* and *D2Mit247* in both of the CAST/Ei backcross. Therefore, this YAC contains the breakpoint that defines the distal boundary of the *Ulnaless* locus (Figure 4).

To determine if there was overlap between the *Hoxd*, *D2Mit10* or *D2Mit247* YACs, we performed inverse PCR and isolated the left ends of YACs FF1.F4, FFC.C8, FDZ.A3, and AAR.F5 (Figure 4). We performed Southern blot analysis on genomic DNA from each of the YAC strains digested with *Eco*RI. The left end of FFC.C8 (*FFCL*) recognized itself, as well as four of the YACs isolated by *D2Mit10*, D.35.G6, FBU.E9, FER.H1, and FCP.F9. This result was confirmed by PCR using primers designed from the *FFCL* sequence on genomic YAC DNA. This closed the contig on the proximal side of *Ulnaless* and confirmed that *Evx-2* is oriented toward the centromere (Figure 4). Primers flanking a CA repeat in the left end of FF1.F4 (*FF1L*) were used to PCR from genomic YAC DNA to show that *FF1L* is on FFC.C8, and two of the *D2Mit10* YACs, FBU.E9 and FCP.F9 (Figure 4). This further confirmed overlap between the *Hoxd* contig and the *D2Mit10* contig. Mapping of the CA repeat of *FF1L* in the CAST/Ei and MOLF/Ei backcrosses showed that it did not recombine with *Ulnaless* (Figure 2, B–D). Therefore, the proximal recombination breakpoint must lie centromeric to *FF1L* (Figure 4).

On the distal side of the *Hoxd* cluster, we were also able to close the contig. The left end of FDZ.A3 (*FDZL*) recognized itself and AAR.F5 on the Southern blot con-

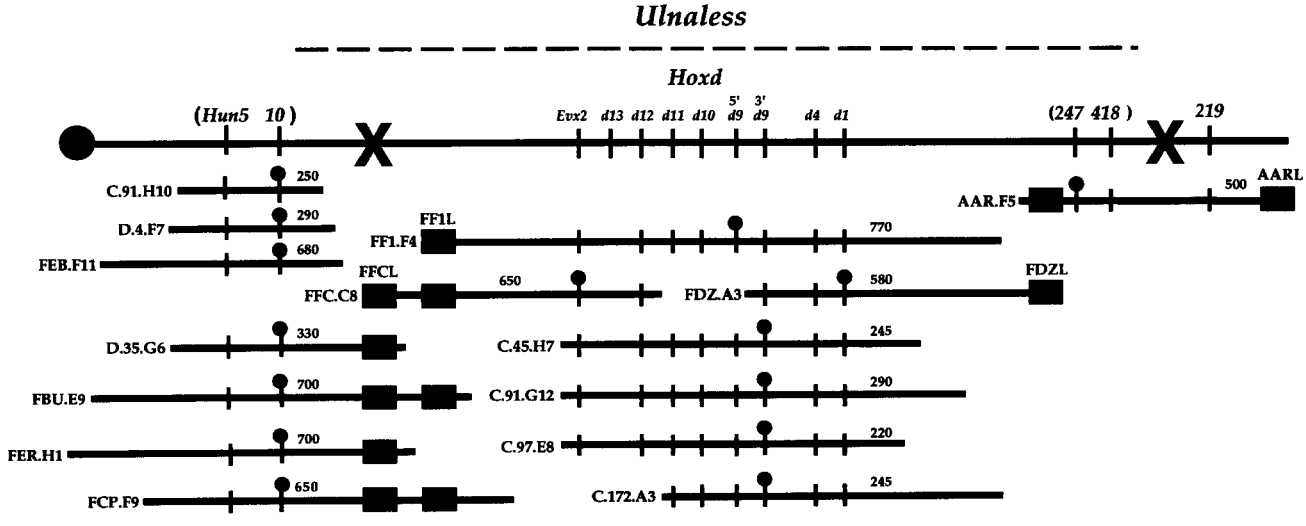

FIGURE 4.—YAC contig of the *Ulnaless* locus. The dashed line indicates the 0.6-cM genetic interval that defines the *Ulnaless* locus. Recombination events are indicated by an X on the schematic chromosome, where the ball indicates the centromere. All markers that were placed on the YACs are indicated on the chromosome. The numbered loci refer to the MIT SSLP markers. Orientation of *D2Hun5* and *D2Mit10* or *D2Mit247* and *D2Mit418* relative to the centromere could not be established; therefore, they are indicated in parenthesis. The YACs are indicated below the chromosome, where vertical lines with balls indicate the marker with which the YAC was isolated, and plain vertical lines indicate other loci that were contained on the YAC. The name of each YAC is to its left and the size in kb of each YAC is indicated over the YAC. The relative location of YAC ends is indicated by solid black boxes.

taining genomic DNA from all of the YAC strains in the *Ulnaless* region. Therefore, the *Hoxd* contig is linked to YAC AAR.F5, which contains the distal breakpoint. The left end of AAR.F5 recognizes only itself on a Southern blot, therefore this end is distal to the breakpoint. Through analysis of the YAC contig, we have defined a 2.08 Mb region containing the *Ulnaless* locus.

DISCUSSION

We have characterized the *Ulnaless* locus on mouse chromosome 2 as a semidominant mutation that affects limb patterning as well as postnatal viability. A high-density genetic map was created using 1564 N_2 animals from four backcrosses, and the *Ulnaless* locus was defined to a 0.4-cM region on mouse chromosome 2. No recombination was observed between *Ulnaless* and the *Hoxd* cluster, suggesting that the *Hoxd* genes are within 0.2 cM of *Ul* (SILVER 1995). Absence of recombination, coupled with the expression of the *Hoxd* genes in the developing limb, and the limb phenotypes associated with targeted mutations in the *Hoxd* genes, suggests that a mutation in a *Hoxd* gene(s) could be responsible for the *Ulnaless* phenotype. The *Ulnaless* interval was cloned using yeast artificial chromosomes and found to span a maximum of 2.0 Mb. The *Hoxd* cluster represents 100 kb of this interval. Although we posit that the genes within this cluster are excellent candidates for allelism with *Ul*, it is possible that the *Ulnaless* mutation resides in another gene within the region.

We characterize *Ulnaless* as a semidominant mutation because the homozygous fore- and hindlimbs are more affected than heterozygous limbs. Although subtle differences between *Ul*/+ and *Ul*/*Ul* animals exist, the *Ulnaless* mutation is rare in that most previously characterized, semidominant mammalian mutations exhibit much more severe effects in the homozygotes, as compared with the heterozygotes (LYON *et al.* 1996). In addition, the *Ulnaless* limb phenotype is 100% penetrant in all four backcrosses with no variable expressivity on either the FVB/N or the MOLF/Ei backgrounds. Perinatal lethality is seen in both *Ul*/+ and *Ul*/*Ul* mice on the FVB/N and CAST/Ei backgrounds, but not the MOLF/Ei background. In contrast to the limb phenotype, perinatal lethality may be dependent upon genetic background and appears to preferentially affect females.

The region of mouse chromosome 2 containing *Ulnaless* has an extended homology to human chromosome *2q24-q37* (SIRACUSA *et al.* 1995), and the human *HOXD* gene cluster has been mapped to *2q31* (ROSSI *et al.* 1994). Therefore, we predict that the human homologue of *Ulnaless* should also map to this region. Intriguingly, an autosomal dominant condition leading to shortened forearms is associated with a balanced translocation involving chromosome *2q32* and *8p23* (VENTRUTO *et al.* 1983; HECHT and HECHT 1984). The limb defects resemble those of a semidominant form of mesomelic dwarfism, dyschondrosteosis, in which there is a greater tendency for females to be affected than males (LICHTENSTEIN *et al.* 1980). Langer mesomelic dwarfism may represent the homozygous state of dyschondrosteosis; however, genetic linkage analysis of these syndromes has not been reported (FRYNS and VAN DEN BERGHE 1979; KUNZE and KLEMM 1980).

Our attention is focused on the *Hoxd* genes as candidates for *Ulnaless*. There are 10 genes in the *Hoxd* cluster contained within 100 kb (BASTIAN *et al.* 1992); however, only the 5′ genes (*Hoxd-8* through *Evx-2*) are expressed in the developing limb (IZPISUA-BELMONTE *et al.* 1990; IZPISUA-BELMONTE and DUBOULE 1992; DOLLE *et al.* 1994). Recently, mutations in two mammalian *Hox* genes have been identified. A human autosomal semidominant condition, syndactyly type II (SynPolyDactyly or SPD) was attributed to an expansion of a polyalanine repeat in the NH_2-terminus of the HOXD13 protein (MURAGAKI *et al.* 1996). The semidominant mouse mutation *Hypodactyly* (*Hd*) is characterized by severe reductions of the distal fore- and hindlimbs in rare surviving homozygotes, and it has been associated with a deletion within the first exon of the *Hoxa-13* gene (MORTLOCK *et al.* 1996).

Targeted mutations in the mouse *Hox* genes also suggest that changes in *Hox* expression in the developing limb lead to reductions and delays in the formation of specific limb structures that can be interpreted to result from heterochronic changes in localized growth rates (DOLLE *et al.* 1993; SMALL and POTTER 1993; DAVIS and CAPECCHI 1994, 1996; DUBOULE 1994; FAVIER *et al.* 1996; FROMENTAL-RAMAIN *et al.* 1996). *Ulnaless* is similar to the *Hox* gene-targeted alleles in that it also appears to reduce and delay growth of specific limb elements. However, *Ulnaless* does not resemble the loss-of-function phenotype in any of the *Hoxa* or *Hoxd* genes in the following respects: the intermediate elements of the limb (ulna and radius) are specifically and severely affected; both the fore- and hindlimbs are affected; and there are no axial skeletal defects. Therefore, we conclude that *Ulnaless* does not simply correspond to the single gene-targeted alleles in *Hoxd-9, Hoxd-11, Hoxd-12,* or *Hoxd-13*. Instead, we propose that *Ulnaless* may specifically affect limb expression of more than one *Hox* gene. This is supported by the fact that mice which are mutant for both *Hoxa-11* and *Hoxd-11* are completely missing the ulna and radius, with less severe defects of the fibula and tibia (DAVIS *et al.* 1995).

Identification of the molecular nature of the *Ulnaless* mutation may lead to insight of the coordinate regulation and complex interactions of *Hox* genes, both within a cluster and across paralogous clusters, and should help define the molecular mechanisms underlying the coordination of proximal-distal and anterior-posterior patterning of the limb.

We thank Dr. P. CHAMBON for the *Hoxd* probes; Dr. P. GRUSS for *Evx-2* sequence; L. ROWE and M. BARTER for The Jackson Laboratory Backcross panels; Dr. K. HUNTER for the *D2Hun5* clone; and J. EHRLICH, J. LEVORSE, and E. MORTON-BOURS for assistance. C.M.A thanks D. CHAMBERS and V. RINALDI for excellent technical assistance. We thank Drs. M. CAPECCHI, A. P. DAVIS, D. DUBOULE, C. TABIN and E. WIESCHAUS for discussions of *Hox* genes and *Ulnaless*; Dr. D. METALLINOS for advice on YACs; Drs. J. MILLONIG, T. O'BRIEN, C. RAUSKOLB, L. SILVER, and S. TILGHMAN for comments on the manuscript; and members of the TILGHMAN and VOGT labs for discussions and support. C.L.P. was supported by the National Institutes of Health Predoctoral Training Program in Genetics. C.M.A. was supported by the U.K. Medical Research Council Human Genome Mapping Project. This research program was initiated and aided by support from the Searle Scholars Program/The Chicago Community Trust to T.F.V. This research in T.F.V.'s laboratory was supported by grants HD-30707 from the National Institutes of Health and DB-143 from The American Cancer Society.

LITERATURE CITED

BASTIAN, H., P. GRUSS, D. DUBOULE and J.-C. IZPISUA-BELMONTE, 1992 The murine even-skipped-like gene *Evx-2* is closely linked to the *Hox-4* complex, but is transcribed in the opposite direction. Mammal. Genome **3:** 241–243.

BULFONE, A., H.-J. KIM, L. PUELLES, M. H. PORTEUS, J. F. GRIPPO *et al.*, 1993 The mouse *Dlx-2* (*Tes-1*) gene is expressed in spatially restricted domains of the forebrain, face, and limbs in midgestation mouse embryos. Mech. Dev. **40:** 129–140.

CARLE, G. F., and M. V. OLSON, 1985 An electrophoretic karyotype for yeast. Proc. Natl. Acad. Sci. USA **82:** 3756–3760.

CROSSLEY, P. H., G. MINOWADA, C. A. MACARTHUR and G. R. MARTIN, 1996 Roles for *Fgf8* in the induction, initiation, and maintenance of chick limb development. Cell **84:** 127–136.

DAVIS, A. P., and M. CAPECCHI, 1994 Axial homeosis and appendicular skeletal defects in mice with a targeted disruption of *hoxd-11*. Development **120:** 2187- 2198.

DAVIS, A. P., and M. CAPECCHI, 1996 A mutational analysis of the 5′ *HoxD* genes: dissection of genetic interactions during limb development in the mouse. Development **122:** 1175–1185.

DAVIS, A. P., D. P. WITTE, H. M. HSIEH-LI, S. S. POTTER and M. R. CAPECCHI, 1995 Absence of radius and ulna in mice lacking *hoxa-11* and *hoxd-11*. Nature **375:** 791–795.

DAVISSON, M. T., and B. M. CATTANACH, 1990 The mouse mutation *Ulnaless* on chromosome 2. J. Hered. **81:** 151–153.

DEL SAL, G., G. MANFIOLETTI and C. SCHNEIDER, 1989 The CTAB-DNA precipitation method: a common mini-scale preparation of template DNA from phagemids, phages, or plasmids suitable for sequencing. BioTechniques **7:** 514–519.

DIETRICH, W. F., J. MILLER, R. STEEN, M. A. MERCHANT, D. DAMRON-BOLES *et al.*, 1996 A comprehensive map of the mouse genome. Nature **380:** 149- 152.

DOLLE, P. J.-C. IZPISUA-BELMONTE, E. BONCINELLI and D. DUBOULE, 1991 The Hox-4.8 gene is localized at the 5′ extremity of the Hox-4 complex and is expressed in the most posterior parts of the body during development. Mech. Dev. **36:** 3–13.

DOLLE, P., M. PRICE and D. DUBOULE, 1992 Expression of the murine *Dlx-1* homeobox gene during facial, ocular, and limb development. Differentiation **49:** 93–99.

DOLLE, P., A. DIERICH, M. LEMEUR, T. SCHIMMANG, B. SCHIBAUR *et al.*, 1993 Disruption of the *Hoxd-13* gene induces localized heterochrony leading to mice with neotenic limbs. Cell **75:** 431–441.

DOLLE, P., V. FRAULOB and D. DUBOULE, 1994 Developmental expression of the mouse *Evx-2* gene: relationship with the evolution of the HOM/Hox complex. Development **Suppl.:** 143–153.

DUBOULE, D., 1994 Temporal colinearity and the phylotypic progression: a basis for stability of a vertebrate Bauplan and the evolution of morphologies through heterochrony. Development **Suppl.:** 135–142.

DUBOULE, D., and P. DOLLE, 1989 The structural and functional organization of the murine HOX gene family resembles that of the *Drosophila* homeotic genes. EMBO J. **8:** 1497–1505.

DUSH, M. K. and G. R. MARTIN, 1992 Analysis of mouse *Evx* genes: *Evx-1* displays graded expression in the primitive streak. Dev. Biol. **151:** 273- 287.

FAVIER, B., F. M. RIJLI, C. FROMENTAL-RAMAIN, V. FRAULOB, P. CHAMBON *et al.*, 1996 Functional cooperation between the non-paralogous genes *Hoxa-10* and *Hoxd-11* in the developing forelimb and axial skeleton. Development **122:** 449–460.

FEATHERSTONE, M. S., A. J. BARON, S. J. GAUNT, M. -G. MATTEI and D. DUBOULE, 1988 *Hox-5.1* defines a homeobox-containing gene locus on mouse chromsome 2. Proc. Natl. Acad. Sci. USA **85:** 4760–4764.

FROHMAN, M. A., and G. R. MARTIN, 1992 Isolation and analysis of embryonic expression of *Hox-4.9*, a member of the murine labial-like gene family. Mech. Dev. **38:** 55–67.

FROMENTAL-RAMAIN, C., X. WAROT, S. LAKKARAJU, B. FAVIER., H. HAACK *et al.*, 1996 Specific and redundant functions of the paralogous *Hoxa-9* and *Hoxd-9* genes in forelimb and axial skeleton patterning. Development **122:** 461–472.

FRYNS, J. P., and H. VAN DEN BERGHE, 1979 Langer type of mesomelic dwarfism as the possible homozygous expression of dyschondrosteosis. Hum. Genet. **46:** 21–27.

GERARD, M., D. DUBOULE and J. ZAKANY, 1993 Structure and activity of regulatory elements involved in activation of the *Hoxd-11* gene during late gastrulation. EMBO J. **12:** 3539–3550.

HECHT, F., and B. K. HECHT, 1984 Linkage of skeletal dysplasia gene to t(2;8)(*q32:3p13*) chromosome translocation breakpoint. Am. J. Med. Genet. **18:** 779–780.

HOFFMAN, C. S., and F. WINSTON, 1987 A ten-minute DNA preparation from yeast efficiently releases autonomous plasmids for transformation of *Escherichia coli*. Gene **57:** 267–272.

IZPISUA-BELMONTE, J.-C., and D. DUBOULE, 1992 Homeobox genes and pattern formation in the vertebrate limb. Dev. Biol. **152:** 26–36.

IZPISUA-BELMONTE, J.-C., P. DOLLE, A. RENUCCI, V. ZAPPAVIGNA, H. FALKENSTEIN *et al.*, 1990 Primary structure and embryonic expression pattern of the mouse *Hox4.3* homeobox gene. Development **100:** 733–746.

IZPISUA-BELMONTE, J.-C., H. FALKENSTEIN, P. DOLLE, A. RENUCCI and D. DUBOULE, 1991 Murine genes related to the *Drosophila AbdB* homeotic genes are sequentially expressed during development of the posterior part of the body. EMBO J. **10:** 2279–2289.

JACKSON LABORATORY BACKCROSS DNA PANEL MAPPING RESOURCE, 1996 http://www.jax.org/resources/document/cmdata

JOHNSON, R. L., R. D. RIDDLE and C. J. TABIN, 1994 Mechanisms of limb patterning. Curr. Opin. Genet. Dev. **4:** 535–542.

KADOMATSU, K., R. P. HUANG, T. SUGANUMA, F. MURATA and T. URAMATSU, 1990 A retinoic acid responsive gene MK found in the teratocarcinoma system is expressed in spatially and temporally controlled manner during mouse embryogenesis. J. Cell. Biol. **110:** 607–616.

KUNZE, J., and T. KLEMM, 1980 Mesomelic dysplasia, type Langer-a homozygous state for dyschondrosteosis. Eur. J. Pediat. **134:** 269–272.

KUSUMI, K., J. S. SMITH, J. A. SEGRE, D. S. KOOS and E. S. LANDER, 1993 Construction of a large insert yeast artificial chromosome (YAC) library of the mouse genome. Mammal. Genome **4:** 391–392.

LAUFER, E., C. E. NELSON, R. L. JOHNSON, B. A. MORGAN and C. J. TABIN, 1994 *Sonic hedgehog* and *Fgf-4* act through a signaling cascade and feedback loop to integrate growth and patterning of the developing limb bud. Cell **79:** 993–1003.

LICHTENSTEIN, J. R., M. SUNDAREM, and R. BURDGE, 1980 Sex-influenced expression of Madelung's deformity in a family with dyschondrosteosis. J. Med. Genet. **17:** 41–43.

LYON, M. F., S. RASTAN and S. D. M. BROWN, 1996 *Genetic Variants and Strains of the Laboratory Mouse.* Oxford University Press, New Oxford.

MCCARTHY, L., K. HUNTNER, L. SCHALKWYK, L. RIBA, S. ANSON *et al.*, 1995 Efficient high-resolution genetic mapping of mouse interspersed repetitive sequence PCR products, toward integrated genetic and physical mapping of the mouse genome. Proc. Natl. Acad. Sci. USA **92:** 5302–5306.

MORRIS, T., 1967 New mutants. Mouse News Letter **36:** 34.

MORTLOCK, D. P., L. C. POST and J. W. INNIS, 1996 The molecular basis of hypodactyly (*Hd*): a deletion in *Hoxa13* leads to arrest of digital arch formation. Nat. Genet. **13:** 284–289.

MURAGAKI, Y., S. MUNDLOS, J. UPTON and B. R. OLSEN, 1996 Altered growth and branching patterns in synpolydactyly caused by mutation in HOXD13. Science **272:** 548–551.

NAGAMINE, C. M., K. CHAN, C. A. KOZAK and Y.-F. LAU, 1989 Chromosome mapping and expression of a putative testis-determining gene in mouse. Science **243:** 80–83.

O'BRIEN, T. P., D. L. METALLINOS, H. CHEN, M. K. SHIN and S. M. TILGHMAN, 1996 Complementation mapping of skeletal and central nervous system abnormalities in mice of the *piebald* deletion complex. Genetics **143:** 447–461.

OCHMAN, H., A. S. GERBER and D. L. HARTL, 1988 Genetic applications of an inverse polymerase chain reaction. Genetics **120:** 621–623.

PARR, B. A., and A. P. MCMAHON, 1995 Dorsalizing signal *Wnt-7a* required for normal polarity of D-V and A-P axes of mouse limb. Nature **374:** 350–353.

PEICHEL, C. L., S. W. SHERER, L. -C. TSUI, D. R. BEIER and T. F. VOGT, 1993 Mapping the midkine family of developmentally regulated signaling molecules. Mammal. Genome **4:** 632–638.

RENUCCI, A., V. ZAPPAVIGNA, J. ZAKANY, J.-C. IZPISUA-BELMONTE, K. BURKI *et al.*, 1992 Comparison of mouse and human *HOX-4* complexes defines conserved sequences involved in the regulation of *Hox4.4*. EMBO J. **11:** 1459–1468.

ROBINSON, G. W., S. WRAY and K. A. MAHON, 1991 Spatially restricted expression of a new family of murine distal-less homeobox genes in the developing forebrain. New Biol. **3:** 1183–1194.

ROSSI, E., A. FAIELLA, M. ZEVIANI, S. LABEIT, G. FLORIDIA *et al.*, 1994 Order of six loci at *2q24-q31* and orientation of the *HOXD* locus. Genomics **24:** 34–40.

ROSSI, J., D. T. BURKE, J. C. M. LEUNG, D. S. KOOS, H. CHEN *et al.*, 1992 Genomic analysis using a yeast artificial chromosome library with mouse DNA inserts. Proc. Natl. Acad. Sci. USA **89:** 2456–2460.

ROWE, L. B., J. H. NADEAU, R. TURNER, W. N. FRANKEL, V. A. LETTS *et al.*, 1994 Maps from two interspecific backcross DNA panels available as a community genetic mapping resource. Mammal. Genome **5:** 253–274.

SILVER, L. M., 1995 *Mouse Genetics: Concepts and Applications*. Oxford University Press, New York.

SIMEONE, A., D. ACAMPORA, M. PANNESE, M. D'ESPOSITO, A. STORNAIULO *et al.*, 1994 Cloning and characterization of two members of the vertebrate *Dlx* gene family. Proc. Natl. Acad. Sci. USA **91:** 2250–2254.

SIRACUSA, L. D., J. L. MORGAN, J. K. FISHER, C. M. ABBOTT, and J. PETERS, 1995 Chromosome 2. 1995 Chromosome Committee Reports. http://linus.informatics.jax.org/ccr/

SMALL, K. M., and S. S. POTTER, 1993 Homeotic transformations and limb defects in *HoxA11* mutant mice. Genes Dev. **7:** 2318–2328.

SUMMERBELL, D., J. H. LEWIS and L. WOLPERT, 1973 Positional information in chick limb morphogenesis. Nature **244:** 492–495.

TICKLE, C., 1995 Vertebrate limb patterning. Curr. Opin. Genet. Dev. **5:** 478–484.

VENTRUTO, V., R. PISCIOTTA, S. RENDA, B. FESTA, M. M. RINALDI *et al.*, 1983 Multiple skeletal familial abnormalities associated with balanced reciprocal translocation 2;8 (*q32:p13*). Am. J. Med. Genet. **16:** 589–594.

YANG, Y., and L. NISWANDER, 1995 Interaction between the signaling molecules *Wnt7A* and *Shh* during vertebrate limb development: dorsal signals regulate anteroposterior patterning. Cell **80:** 939–947.

Communicating editor: K. ARTZT